

# Domain Embedded Multi-model Generative Adversarial Networks for Image-based Face Inpainting

Xian Zhang <sup>\*1</sup>, Xin Wang <sup>\*\*2</sup>, Bin Kong<sup>2</sup>, Youbing Yin<sup>2</sup>, Qi Song<sup>2</sup>, Siwei Lyu<sup>3</sup>, Jiancheng Lv<sup>5</sup>, Canghong Shi<sup>4</sup>, Xi Wu<sup>1</sup>, and Xiaojie Li<sup>†1</sup>

<sup>1</sup>Chengdu University of Information Technology

<sup>2</sup>CuraCloud Corporation

<sup>3</sup>SUNY Albany

<sup>4</sup>Southwest Jiaotong University

<sup>5</sup>SiChuan University

## Abstract

Prior knowledge of face shape and location plays an important role in face inpainting. However, traditional facing inpainting methods mainly focus on the generated image resolution of the missing portion but without consideration of the special particularities of the human face explicitly and generally produce discordant facial parts. To solve this problem, we present a stable variational latent generative model for large inpainting of face images. We firstly represent only face regions with the latent variable space but simultaneously constraint the random vectors to offer control over the distribution of latent variables, and combine with the non-face parts textures to generate a face image with plausible contents. Two adversarial discriminators are finally used to judge whether the generated distribution is close to the real distribution or not. It can not only synthesize novel image structures but also explicitly utilize the latent space with Eigenfaces to make better predictions. Furthermore, our work better evaluates the side face inpainting problem. Experiments on both CelebA and CelebA-HQ face datasets demonstrate that our proposed approach generates higher quality inpainting results than existing ones.

## 1. Introduction

Image inpainting refers to the task of filling in missing or masked regions with synthesized contents. Among the various ways of vision algorithm of today, deep learning based methods have attracted a lot of attention in im-

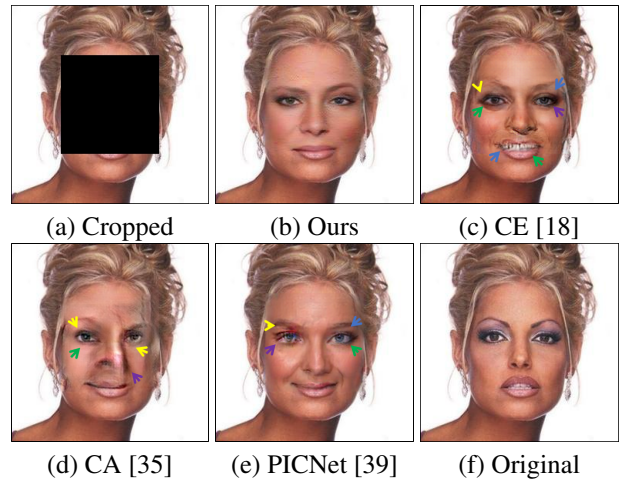


Figure 1. Challenging example handled by previous approaches. (a) cropped image (f)original image. In result (c), the facial part has fuzzy boundaries and details (purple arrow), which is not visually-realistic. In results (d) and (e), some parts are not structurally-reasonable, e.g. the eyebrow (yellow arrow) are asymmetry, the eyes (green arrow) have different size. Our result (b) shows excellent performance on texture and facial structure.

age inpainting. The earliest deep learning image inpainting method was called context encoders (CE) by Deepak Pathak et al [18]. They compulsively obtain latent characteristic information of the missing area by context information. However, the context encoders only pay attention to the missing area information rather than the whole image such that the generated image would have obvious patching marks at the boundary (see Fig. 1(c)). To solve the problem, Yu et. al. proposed generative image inpainting with contextual attention (CA) [35], it first generated a low-

\*indicates equal contribution

†Corresponding author

resolution image in the missing area, then updated the refinement image by searching for patches similar to an unknown area from a known area with contextual attention. Zheng et. al. proposed a pluralistic image completion network (PICNet) with a reconstructive path and the generative path to creating multiple plausible results [39]. However, all these methods produce discordant facial parts, which are not structurally-reasonable. For example, the asymmetry eyebrow (see Fig. 1(d)), one eye is large and the other one is small (see Fig. 1(e)) or two eyes of one people have different colors (see Fig. 1(e)).

One possible reason is that these general image inpainting methods mainly focus on the generated image resolution of the missing portion and consider its conformance with the external context but without consideration of the special particularities of the human face (e.g., symmetrical relation, harmonious relation) in their approach. Only a few works [11, 13] dedicated to the task of face inpainting. These face inpainting algorithms incorporate simple face features into a generator for human face completion. However, the benefit of face region domain information has not been fully explored, which also leads to unnatural images. Face inpainting remains a challenging problem as it requires to generate semantically new pixels for the missing key components with consistency on structures and appearance.

In this paper, A Domain Embedded Multi-model Generative Adversarial Network (DEGNet) is proposed for face inpainting. We firstly embedding the face region domain information (i.e., face mask, face part and landmark image) by variational auto-encoder into a latent variable space as the guidance, where only face features lie in the latent variable space. Before generating a face image with plausible contents, we combine the face region domain embedded latent variable into the generator for face inpainting. Finally, our adversarial discriminators judge whether the generated face image is close to the real distribution or not. Experiments on two benchmark face datasets [15, 10] demonstrate that our proposed approach generates higher quality inpainting results than the state-of-the-art methods. The main contributions of this paper are summarized as follows:

- Our proposed model embedding the face region information into latent variables as the guidance information for face inpainting. The proposed method enables complex real scenes learning and produces sharper and more natural faces, and thus leads to improved face structure prediction, especially for larger missing regions.
- We design a new learning scheme with the patch and global adversarial loss, in which the global discriminator could control the overall spatial consistency and the patch discriminator could provide more elaborate

face feature distribution which can generate impressively photorealistic high-quality face images.

- To the best of our knowledge, our work is the first on the evaluation of the side face inpainting problem, and more importantly our inpainting results of side face show excellent visual quality and facial structures comparing to the state-of-the-art methods.

## 2. Related Work

**General Image Inpainting.** Traditional diffusion-based or patch-based methods [3, 4, 31, 9] with low-level features generally assume image holes share similar content to visible regions; thus they would directly match, copy and realign the background patches to complete the holes. These methods perform well for background completion, e.g. for object removal, but cannot hallucinate unique content not present in the input images. Barnes et al. [2] proposed a fast nearest-neighbor field algorithm called PatchMatch (PM) for image editing applications including inpainting. It greatly reduces the search scopes of patch similarity by utilizing the continuity of images. Based on the nearest neighbor (NN) inpainting method, Whyte et al. [27] updated the predicted region by finding the nearest image from the original image in the training data set. While the above methods become less effective when the missing region becomes large or irregular.

Many recent image inpainting methods are proposed based on deep learning model [6, 33, 14, 32, 20, 7, 29]. Li et al. [12] propose a deep generative network for face completion, it consists of an encoding-decoding generator and two adversarial discriminators to synthesize the missing contents from random noise. The proposed model[30, 23, 32, 26, 36] can synthesize plausible contents for the missing facial key parts from random noise. Alternatively, given a trained generative model, Raymond et al. [34] search for the closest encoding of the corrupted image in the latent image manifold using their context and prior losses to infer the missing content by the generative model. To recover large missing areas of an image, Patricia et al. [24] tackle the problem not only by using the available visual data but also by taking advantage of generative adversarial networks incorporating image semantics. However, these methods can generate visually plausible image structures and textures, but usually, create distorted structures or blurry textures inconsistent with surrounding areas.

To reduce the blurriness issue commonly existing in the CNN-based inpainting, two-stage methods have been proposed to conduct texture refinement on the initially completed images [38, 35, 23]. Generally, they firstly filled the missing regions by a content generation network and then updated the neural patch in the predicted region with fine

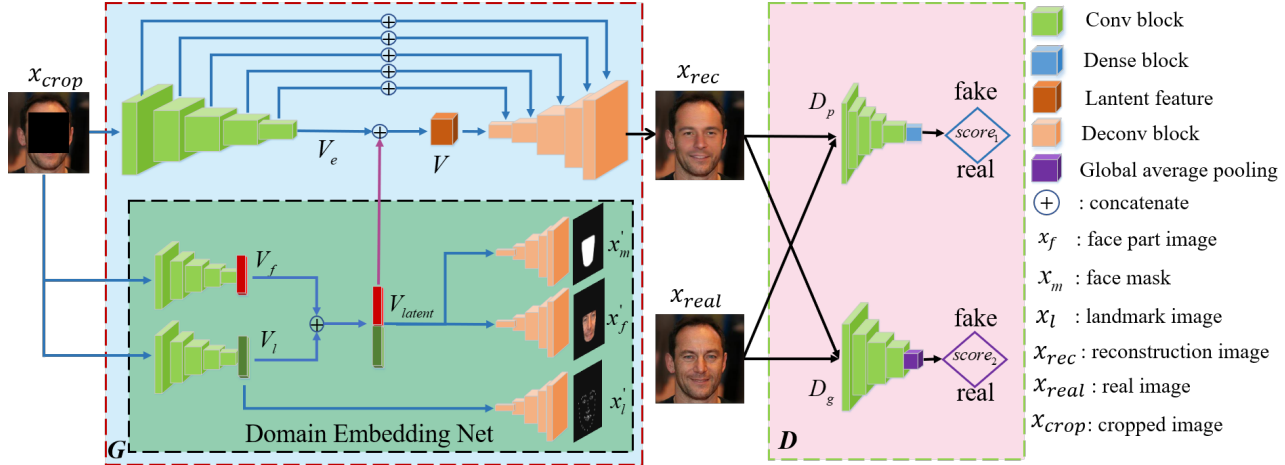


Figure 2. Overview of the DEGAN architecture, it mainly consists of three modules: Domain Embedding Net, Domain Embedded Generator (G) and Multi-model Discriminators (D), i.e.  $D_g$  (global discriminator) and  $D_p$  (patch discriminator).

textures in the known region. Recently Yu et al. [35] propose a new deep generative model-based approach for inpainting. It not only synthesizes novel image structures but also explicitly utilizes surrounding image features as references to make better predictions. While it is likely to fail when the source image does not contain a sufficient amount of data to fill in the unknown regions. When the training image is a Non-HQ image, it performs not well. Furthermore, such processing might introduce undesired content change in the predicted region, especially when the desired content does not exist in the known region. To avoid generating such in-correct content, Xiao et al. [28] propose a content inference and style imitation network for image inpainting. It explicitly separates the image data into content code and style code to generate the complete image. It performs well on structural and natural images in terms of content accuracy as well as texture details but does not demonstrate its performance on face image inpainting. Zheng et al. [39] present a pluralistic image completion approach for generating multiple and diverse plausible solutions for image completion. However, it cannot keep stable performance and needs a sufficiently varied high-quality dataset.

**Face Inpainting.** Li et al. proposed a deep generative face inpainting model that consists of an encoding-decoding generator, two adversarial discriminators, and a parsing network to synthesize the missing contents from random noise. To ensure pixel faithfulness and local-global contents consistency, they use an additional semantic parsing network to regularize the generative networks (GFCNet) [11]. In 2018, under a novel generative framework called collaborative GAN (collagen) [13], Liao et al. proposed a collaborative adversarial learning approach to facilitate the direct learning of multiple tasks including face completion, landmark detection and semantic segmentation for better seman-

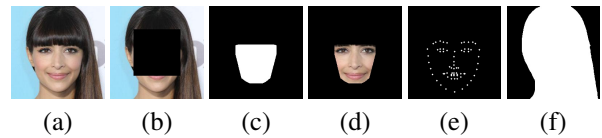


Figure 3. Our method uses six types of images, (a) Original image, (b) Cropped image, (c) Face mask image, (d) Face part image, (e) Face landmark image, (f) Face foreground mask image.

tic understanding to ultimately yield better face inpainting.

### 3. Domain Embedded Multi-model GAN

An overview of our proposed framework is shown in Fig. 2. Our goal is to use the domain information of the face part to generate high quality face inpainting images. We first introduce our Face Domain Embedded Generator and Multi-model Discriminator in Section 3.1 and Section 3.2, respectively. Finally, the loss functions of these components are described in Section 3.3. Note that the details of network structure (number of layers, size of feature maps etc.) can be found in the supplementary document (see Table A1).

#### 3.1. Face Domain Embedded Generator

**Domain Embedding Network.** Given a face image  $x_{real}$  randomly drawn from the training set and its cropped image  $x_{cropped}$ , our goal is to learn the most important face domain information to guide the inpainting procedure. We use face region images which include face mask image  $x_m$  and face part image  $x_f$  and face landmarks image  $x_l$  to represent the face domain information, see Fig.3 (c,d,e).

Then, we use a VAE network [5, 19, 16] with an encoder-decoder architecture to embed the face domain information into latent variables. More specifically, in the encoding phase, the corrupted face image  $x_{cropped}$  is first passed to

two encoders, face region encoder and face land mark encoder, yielding standard normal distributions for the face region image and face landmarks image, respectively. Subsequently, latent variables are sampled from each of these two normal distributions:

$$\begin{aligned} V_f &\sim \mathcal{N}(\mu_f, \sigma_f) \\ V_l &\sim \mathcal{N}(\mu_l, \sigma_l) \end{aligned} \quad (1)$$

where  $V_f$  and  $V_l$  are the sampled latent variables for the face region and face landmarks, respectively.  $\mu_\alpha$  and  $\sigma_\alpha$  with  $\alpha \in \{f, l\}$  denote the means and variances of the generated standard normal distributions.

In the decoding phase,  $V_f$  and  $V_l$  are concatenated to  $V_{latent}$ . The face mask decoder and face part decoder takes  $V_{latent}$  as input and generate the reconstructed face mask  $x'_m$ , face part image  $x'_f$ , and the face landmark decoder take  $V_l$  as input and generate the reconstructed face landmark image  $x'_l$  (See Fig.2). During the training process, the above crucial face information is embedded into the latent variable  $V_{latent}$ . The structure of these two encoders are symmetrical to that of the three decoders and all of them have different weights.

**Domain Embedded Generator.** To reconstruct the complete and harmonious face image, we need to integrate the embedded latent variable  $V_{latent}$  into the face Generator. We use Unet [21] as our generator, in the encoding phase, the cropped image  $x_{cropped}$  is sent into Unet and get a latent feature  $V_e$  with size (16, 16, 512) from the middle layer of the Unet. To concatenate  $V_{latent}$  and  $V_e$ , we resize  $V_{latent}$  into (16, 16, 2) and concatenate  $V_e$  and  $V_{latent}$  on their last channels, denote as  $V$ . In the decoding phase, we generate realistic face images by deconvolution blocks with  $V$  as input, See Fig. 2.

### 3.2. Multi-model Discriminator

In our network, the generator would produce blurry face images without discriminator. So we use a global-discriminator to get a clear face image. We use patch-discriminator from PatchGAN [8] to enhance image quality. In particular, when generating face image  $x_{rec}$ , we put  $x_{rec}$  with  $x_{real}$  into two discriminator to distinguish true or fake. In DEGNet, we adopt a global discriminator to guarantee the spatial consistency of the global structure of  $x_{rec}$  with  $x_{real}$  in the beginning process. When  $x_{rec}$  with  $x_{real}$  has been consistent with the overall spatial structure, patch discriminator then split  $x_{rec}$  into patches to refine the spatial structure consistent with  $x_{real}$  on every patch. In addition to producing realistic face image, Not only can we enhance the robustness and generalization performance of the generator, but also the Domain Embedding Net achieves more abundant and accuracy before face information in the cropped region by two discriminators influence.

#### Algorithm 1

*DEGNet Algorithm.* All experiments in this paper set  $\alpha = 0.0002$ ,  $m = 64$

**Require:** :  $\alpha$ : learning rate,  $m$ : batch size,  $W_{vae}$ : Vae's parameters,  $W_u$ : Unet's parameters,  $W_g$ : global-discriminator parameters,  $W_p$ : patch-discriminator parameters,  $V_{latent}$ : sampled latent vector from Vae's encoder,  $X_{prior}$ : domain information about face,  $D_p$ : patch-discriminator,  $D_g$ : global-discriminator

```

1: while  $W_{vae}$  and  $W_u$  have not converged do
    $V_{latent}^{(i)} \sim \text{sample}\{x_{cropped}^{(i)}\}_{i=1}^m$ : sample a batch from the cropped data
    $x_m, x_f, x_l \sim G\{V_{latent}^{(i)}, V_l^{(i)}\}_{i=1}^m$ : generate facial information from the Vae's decoder
    $x_{rec}^{(i)} \sim G\{x_{cropped}^{(i)}, V_{latent}^{(i)}\}_{i=1}^m$ : reconstructed images by Unet
    $score_1 \sim D_p\{x_{rec}^{(i)}, x_{real}^{(i)}\}_{i=1}^m$ : discriminate the distribution of  $x^{(i)}$  real or fake
    $score_2 \sim D_g\{x_{rec}^{(i)}, x_{real}^{(i)}\}_{i=1}^m$ : discriminate the distribution of  $x^{(i)}$  real or fake
   Update  $W_{vae}$  by  $\mathcal{L}_m^{rec}, \mathcal{L}_f^{rec}, \mathcal{L}_l^{rec}, \mathcal{L}_f^{lat}, \mathcal{L}_l^{lat}$  and  $\mathcal{L}_m^{lat}$ 
   Update  $W_u$  by  $\mathcal{L}_x^{rec}, \mathcal{L}_x^{adv}, \mathcal{L}_p^{adv}$ 
   Update  $W_g$  and  $W_p \sim \{score_1, score_2\}$ 
2: end while

```

**end**

### 3.3. Loss Function

**Domain Embedding Network Loss.** For corrupted face image  $x_{cropped}$ , the VAE network are trained to reconstruct the face mask  $x'_m$ , face region  $x'_f$ , and the landmark image  $x'_l$ . In this work, we define three reconstruction losses (see Eq.(2)) for these three outputs, respectively:

$$\begin{aligned} \mathcal{L}_m^{rec} &= \mathbb{E}[\mathcal{L}_{CE}(x_m, x'_m)] \\ \mathcal{L}_f^{rec} &= \mathbb{E}[\|x_f - x'_f\|_1] \\ \mathcal{L}_l^{rec} &= \mathbb{E}[\mathcal{L}_{CE}(x_l, x'_l)] \end{aligned} \quad (2)$$

where  $\mathcal{L}_{CE}$  denotes the cross-entropy loss, and  $x_m, x_f$ , and  $x_l$  are the corresponding ground truth images. The encoder can extract face domain information more accurately under the constraint of (2). To impose a domain distribution (in our case, the standard normal distribution) on the latent space, we employ a latent classifier  $C_\omega$  rather than the Kullback-Leibler divergence used in standard VAEs. This technique has been demonstrated to help the VAE to capture better data manifold, thereby learning better latent representations [17]. This technique has also been widely used in various VAE-based generative networks such as  $\alpha$ -GAN [22]. The latent classification loss is defined as fol-

lows:

$$\mathcal{L}_f^{lat} = -\mathbb{E}[\log C_\omega(V)] - \mathbb{E}[\log(1 - C_\omega(V_f))] \quad (3)$$

where  $V \sim \mathcal{N}(0, 1)$  is a random variable randomly sampled from the standard normal distribution. Equally  $L_l^{lat}$  and  $L_m^{lat}$  are defined for  $V_l$  and  $V_m$ . where  $V_m$  is the connection of the  $V_f$  with  $V_l$  in the last channels.

**Domain Embedded Generator Loss.** To construct the background information more quickly and make the missing region and its inversion having a better fusion effect indirectly, we impose the following reconstruction loss for the foreground region  $M_{FG}$  that including face and hair regions.

$$\mathcal{L}_x^{rec} = \mathbb{E}[|||(x_{rec} - x_{real}) \otimes (M_{FG} + \beta(1 - M_{FG}))|||_1] \quad (4)$$

where  $||\cdot||_1$  normal can penalty the difference between  $x_{rec}$  and  $x_{real}$ . Remembering capabilities can be further evaluated by the reconstruction accuracy of given sample under its latent representation.

**Multi-model Discriminator Loss.** apart from a normal discriminator (global discriminator)  $D_g$ , a patch discriminator  $D_p$  is introduced to discriminate the reconstructed face image  $x_{rec}$  against the uncorrupted face image  $x_{real}$ . We use global-discriminator and patch-discriminator to be adversarial with face domain embedding generator. We adopt global adversarial loss and patch adversarial loss to learn more better latent representation and encourage the generated images  $x_{rec}$  that look realistic and natural. Therefore, the loss for the face generator is as follows:

$$\begin{aligned} \mathcal{L}^{adv-p} &= -\mathbb{E}[\log(1 - D_p(x_{rec}))] - \mathbb{E}[\log(D_p(x_{real}))] \\ \mathcal{L}^{adv-g} &= -\mathbb{E}[\log(1 - D_g(x_{rec}))] - \mathbb{E}[\log(D_g(x_{real}))] \end{aligned} \quad (5)$$

The former distinguishes whether a local patch of the image is from a real sample or a synthesized image. It has the ability to capture the local statistics and drive the generator to generate locally coherent face images. The latter distinguishes whether an image is a real sample or a synthesized image. This can significantly improve adversarial training robustness and alleviate the transferability among the members of the ensembles in both untargeted and targeted modes.

**Total Loss.** The overall loss function of our model is defined by a weighted sum of the above loss functions:

$$\begin{aligned} \mathcal{L} &= \lambda_f^{rec} \mathcal{L}_f^{rec} + \lambda_m^{rec} \mathcal{L}_m^{rec} + \lambda_l^{rec} \mathcal{L}_l^{rec} \\ &+ \lambda^{lat} (\mathcal{L}_f^{lat} + \mathcal{L}_m^{lat} + \mathcal{L}_l^{lat}) \\ &+ \lambda^{adv-g} \mathcal{L}^{adv-g} + \lambda^{adv-p} \mathcal{L}^{adv-p} \end{aligned} \quad (6)$$

## 4. Experiments

### 4.1. Experiments Settings.

**Datasets.** Our experiments are conducted on two human face data sets. 1) CelebA [15], a Large-scale CelebFaces Attributes Dataset. 2) CelebA-HQ [10], a high-quality version of CelebA dataset. We follow the official split for training, validating and testing (details in Table 1).

Table 1. Training and test splits of two datasets.

Data Set	#Train	#Val	#Test
CelebA [15]	162770	19867	19962
CelebA-HQ [10]	28000	1000	1000

**Evaluation Metrics.** Three types of criteria are used to measure the performance of different methods: 1) Peak Signal to Noise Ratio (PSNR), which directly measures visibility of errors and gives you an average value; 2) Structural SIMilarity (SSIM), which measures the structural similarity of an image against a reference image; 3) Normalization Cross Correlation (NCC), which has been commonly used to evaluate the degree of similarity between two compared images.

**Pre-processing.** Our training dataset includes six types of images (see Figure 3): 1) the original full-face image with  $178 \times 218$  (Figure 3(a)), 2) cropped face image or landmarks (Figure 3(b)), 3) face mask  $M_{\theta-f}$  (Figure 3(c)), 4) face part  $x_{\theta-f}$  (Figure 3(d)), 5) landmark image  $x_{\theta-l}$  (Figure 3(e)), we use face\_alignment detection interface [25] to extract 68 facial landmarks properly from an original full-face image, and 6) foreground mask  $M_{\theta-FG}$  (Figure 3(f)).

The cropped face image (Figure 3(b)) and face mask (Figure 3(c)) are obtained by stretching the convex hull computed from the 41 landmarks in eyes nose and mouth. To obtain face part, we dilate the face mask by 3% of the image width to ensure that the mask borders are slightly inside the face contours and include the eyebrows inside the mask. Then the only face part image (Figure 3(d)) is obtained by applying the face mask to the input image. Finally, the foreground mask (Figure 3(f)) is detected using Baidu segmentation API [1].

All of these face images are coarsely cropped and resized from  $178 \times 218$  to  $178 \times 178$ . Finally, the cropped image will be resized to  $128 \times 128$  in our experiment.

**Implementation Details.** All experiments are implemented using Tensorflow and Keras framework. We use Adam optimizer with an initial learning rate of 0.0002,  $\beta_1 = 0.5$ ,  $\beta_2 = 0.999$  and leave other parameters as Keras default. Our model uses batch size of 60 training with 80 epochs and sets  $\lambda_m^{rec} = \lambda_f^{rec} = 4,000$ ,  $\lambda_l^{rec} = 2,000$ ,  $\lambda^{lat} = 30$  and  $\lambda^{adv-p} = 30$ .

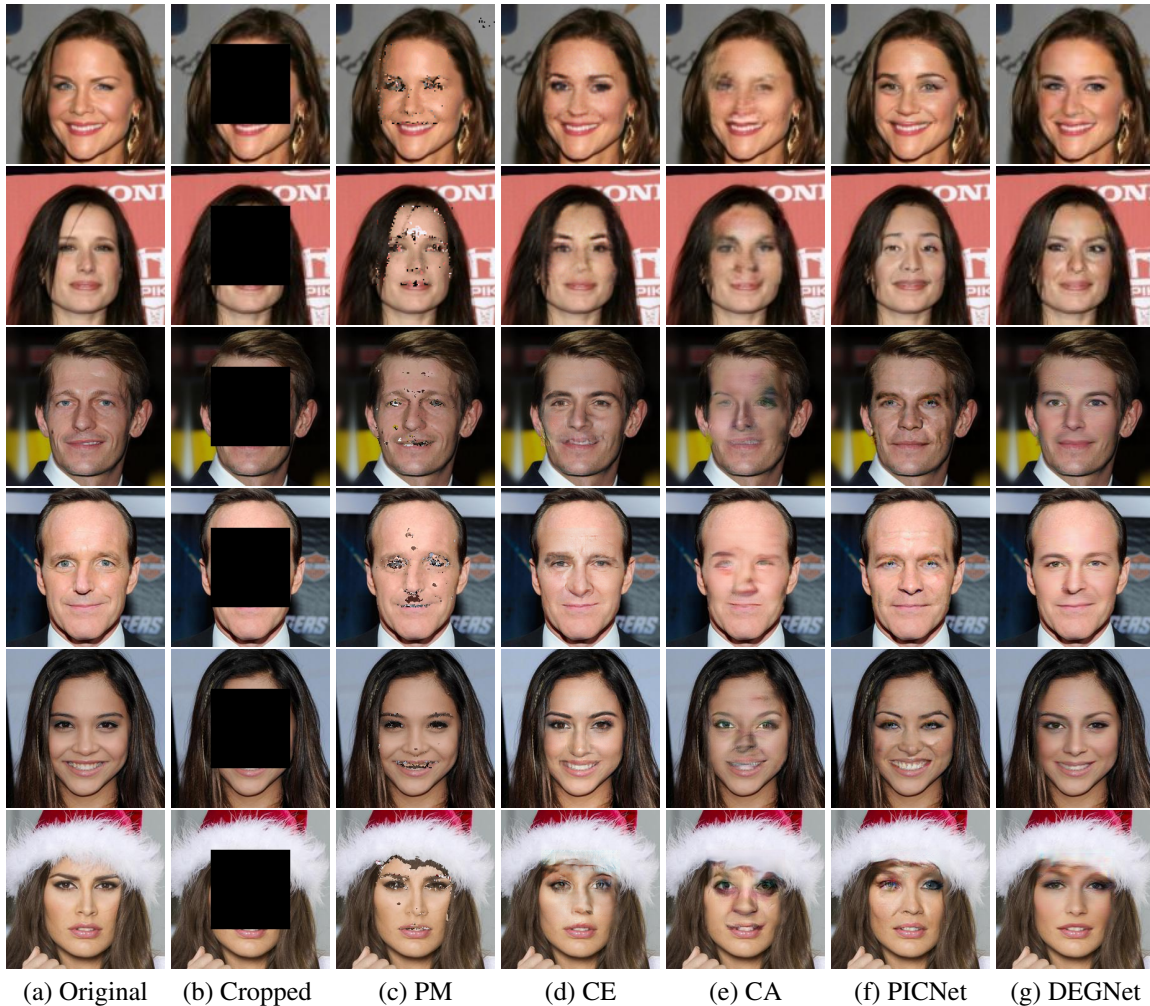


Figure 4. Qualitative results of different inpainting methods on the CelebA dataset (the first two rows) and CelebA-HQ dataset (the rest rows). More examples can be found in the supplementary materials.

Table 2. Comparison of the proposed DEGNet with the other advanced methods on CelebA.

Method	PSNR	SSIM	NCC
PM [2]	22.0	0.861	0.931
CE [18]	24.950	0.870	0.969
CA [35]	23.897	0.858	0.962
PICNet [39]	25.135	0.876	0.970
DEGNet (Our)	<b>25.274</b>	<b>0.882</b>	<b>0.972</b>

Table 3. Comparison of the proposed DEGNet with the other advanced methods on CelebA-HQ.

Method	PSNR	SSIM	NCC	L1-loss
PM [2]	23.190	0.887	0.952	52.02
CE [18]	26.076	0.885	0.978	44.13
CA [35]	22.862	0.844	0.954	47.21
PICNet [39]	25.091	0.869	0.972	44.74
PEN [37]	-	-	-	9.94
DEGNet (Our)	<b>26.208</b>	<b>0.895</b>	<b>0.978</b>	<b>4.65</b>

## 4.2. Comparison with Existing Work

We compare our algorithm against existing works in two groups: general image inpainting methods and face inpainting methods separately:

**1) General image inpainting methods:** The texture refinement methods PM [2], Context\_encoder (CE) [18] and Generative\_inpainting (CA) [35] that replacing the initially completed images and traditional methods which only using

low-level features to complete image inpainting and Pluralistic Network (PICNet) [39], noted that since PICNet can generate multiple outputs, we chose the top one best results based on its discriminator scores to compare. Both PICNet and CA methods require high-resolution training images in original papers, we report their results on the high-resolution CelebA-HQ data set. And there is no public code

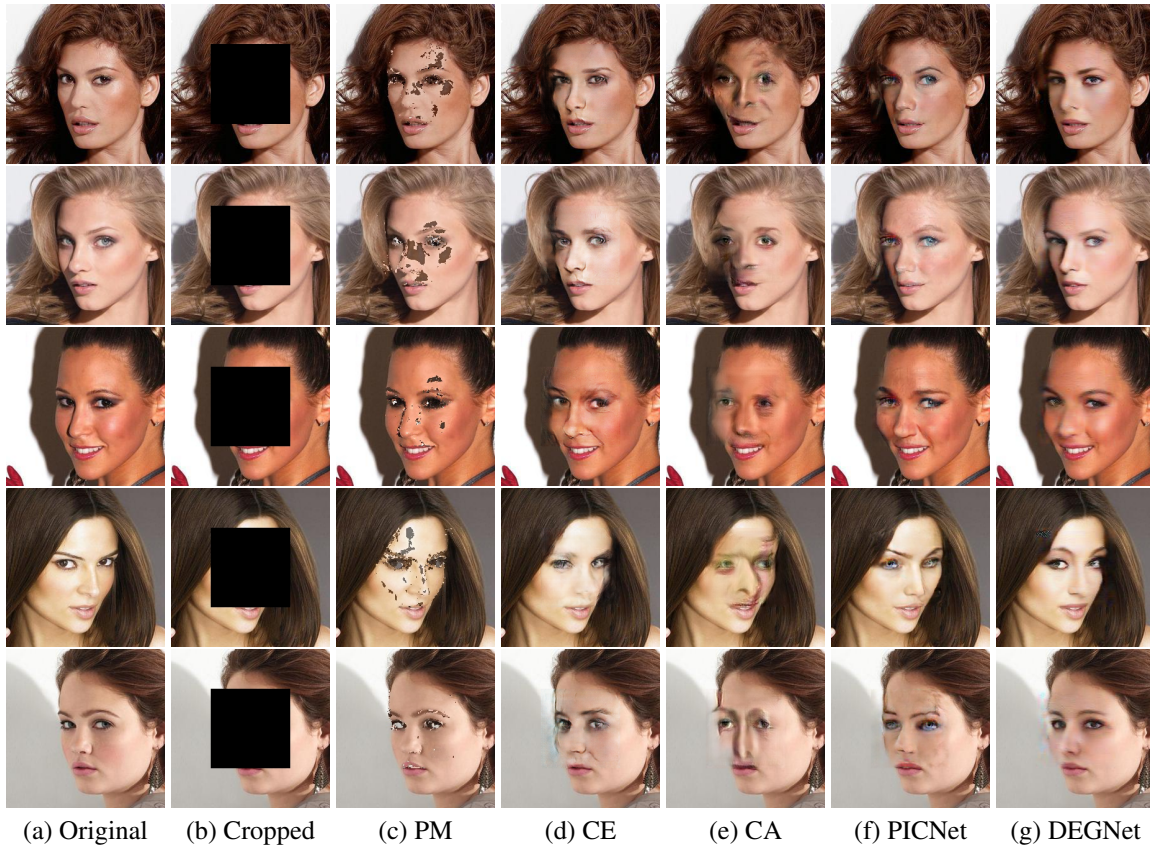


Figure 5. Qualitative results of different inpainting methods on side face. More examples can be found in the supplementary materials.

Table 4. Qualitative face completion comparison of different models with different settings and varying numbers of tasks: left eye (O1), right eye (O2), upper face (O3) left face (O4), right face (O5), and lower face (O6). The numbers are SSIM/PSNR, the higher the better.

Method	O1	O2	O3	O4	O5	O6
CE [18]	0.905/26.74	0.906/27.01	0.938/27.90	0.958/30.37	0.960/30.65	0.90/27.11
GFCNet [11]	0.789/19.7	0.784/19.5	0.759/18.8	0.824/20	0.826/19.8	0.841/20.2
CollarGAN [13]	0.924/27.76	0.926/27.97	0.952/28.79	<b>0.972/31.44</b>	0.972/31.5	0.917/27.81
DEGNet	<b>0.994/39.69</b>	<b>0.994/40.09</b>	<b>0.986/35.50</b>	<b>0.966/31.96</b>	<b>0.975/33.97</b>	<b>0.990/39.14</b>

available for the PENNet [37], we compare the best  $L_1$  loss performance reported in their paper.

**2) Face inpainting methods:** GFCNet [11], and CollaGAN [13]. As there are no public code available for both methods, we report the best performance in their paper. Aiming at fair comparison, our experiments follow their experiments setting and use the same dataset with the same training and testing split.

#### 4.2.1 Quantitative Comparisons.

##### Comparison with General image inpainting methods.

As presented in Fig. 4, the first two lines of inpainting results are from the Celeba, and others are from the Celeba-HQ. When the missing area is quite different from the surrounding environment, we find that PM method does not

inpaint the whole face, and the CE method has better performance in some frontal faces but when the missing area contains some background information besides face, it is a high possibility for CE to produce blurry even distorted face. PIC can inpaint clear faces but the faces are not harmonious. This is because PIC is to produce clearer image by enhance the constraint capability of discriminator, which destroy the structural consistency of the image and result in distortion of the image. In DEGNet, we produce clear and harmonious face inpainting by keep balance between rec loss and adv loss.

As presented in Table 2 and Table. 3, our method in general achieve better performance than all the other methods, in terms of SSIM, PSNR, and NCC. It is easy to see that our method outperforms state-of-the-arts in both PSNR and SSIM and achieves the best generalization performance for



(a) O1 (b) O2 (c) O3 (d) O4 (e) O5 (f) O6

Figure 6. Qualitative face completion comparison of our methods with different masks.

large and different crops. CA only achieve better results for high resolution training dataset, but get poor result for low resolution training dataset (see figure 1(d)).

**Compassion with Face inpainting methods.** In addition comparing to the general image inpainting methods, we also compare to face inpainting methods. As shown in figure 6, we completed all kinds of part cropped face inpainting. We produced clear and natural result. Because of without code and visual feature in thier paper, we only show our feature.

As shown in Table 4, our method in general achieve the better performance over all other methods in terms of SSIM and PSNR. It is easy to find that the values of PSNR and SSIM in our methods are significantly higher than those of CFGNet with CollaGAN except O4.

### 4.3. Evaluation of Side Face Inpainting

Besides frontal face inpainting, we further evaluate face inpainting performance on the side face. Different from the frontal face, the cropped side face contains more missing information. In terms of side face, the facial features information is difficult to learn than the frontal face. So it is hard to complete face inpainting inside face. Generally, most of the existing methods failed on side face inpainting. To illustrate the problem, Table 5 and Fig. 5 shows the quantitative and qualitative comparisons of different methods on side face inpainting. Table 5 shows that our method outperforms state-of-the-art in both PSNR and SSIM on the side face inpainting. From Figure 5, we find that our DEGNet method has symmetry faces, such as eyes with the same sizes and colors, while other methods include blurry textures and asymmetry faces.

Table 5. Comparison of the proposed DEGNet with the other advanced methods on side face.

Method	PSNR	SSIM
PM [2]	24.44	0.873
CE [18]	25.35	0.878
CA [35]	22.4	0.844
PICNet [39]	24.87	0.867
DEGNet (Our)	<b>25.36</b>	<b>0.886</b>

Table 6. Quantitative face completion comparison with large regular holes of our methods with different components: rec (S1), rec+global (S2), and rec+global+patch (S3). Higher values are better.

	S1	S2	S3
PSNR	25.590	23.518	<b>26.208</b>
SSIM	0.886	0.856	<b>0.895</b>

### 4.4. Ablation Study.

We further perform experiments to study the effect of the components of our model. We analyze how the different combinations of our components, (S1) reconstruction, (S2) Reconstruction + global discriminator, (S3) Reconstruction + global discriminator+ patch discriminator, affect our inpainting performance, the results are shown in Table 6 and Fig. 7). Based on our backbone, we further impose the latent classifier on the random vector, which results in better PSNR and SSIM. As an intermediate test, the global discriminator somewhat decreases the SSIM score. Moreover, based on the former, more other two global and patch discriminators only acting on the missing region would result in more better results.

And three constraint factors actually can have a positive effect on their performance development. According to our previous analysis, we know that reconstruction constraints and discriminator can improve the performance of our backbone directly. We also explored different training modes on how to affect its performance. Thus combing with domain embedded generator and discriminator alternative optimization, our DEGNet is proposed to overcome this problem and discuss how to generate high-quality face inpainting images based on this.

## 5. Conclusion

We proposed a Domain Embedded Multi-model Generative Adversarial Network for face image inpainting. Our proposed model improves the face inpainting performance by using the face region information as the guidance information within a Multi-model GAN framework. Experimental results demonstrate our method gets better performance than the state-of-the-art face inpainting methods. Furthermore, our method could be easily applied to other image editing tasks.

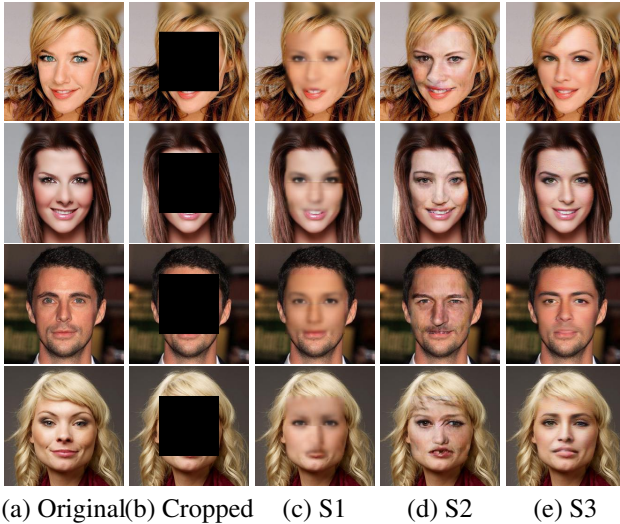


Figure 7. Qualitative face completion comparison of our methods with different components S1, S2 and S3 and total loss.

## References

- [1] Baidu. <https://ai.baidu.com/tech/body/seg>, 2019.
- [2] Connelly Barnes, Eli Shechtman, Adam Finkelstein, and Dan B Goldman. Patchmatch: A randomized correspondence algorithm for structural image editing. In *ACM Transactions on Graphics (ToG)*, volume 28, page 24. ACM, 2009.
- [3] Marcelo Bertalmio, Guillermo Sapiro, Vincent Caselles, and Coloma Ballester. Image inpainting. In *Proceedings of the 27th annual conference on Computer graphics and interactive techniques*, pages 417–424. ACM Press/Addison-Wesley Publishing Co., 2000.
- [4] Antonio Criminisi, Patrick Pérez, and Kentaro Toyama. Region filling and object removal by exemplar-based image inpainting. *IEEE Transactions on Image Processing*, 13(9):1200–1212, 2004.
- [5] Carl Doersch. Tutorial on variational autoencoders. *arXiv preprint arXiv:1606.05908*, 2016.
- [6] Kaiming He, Xiangyu Zhang, Shaoqing Ren, and Jian Sun. Deep residual learning for image recognition. In *Proceedings of the IEEE Conference on Computer Vision and Pattern Recognition (CVPR)*, pages 770–778, 2016.
- [7] Xin Hong, Pengfei Xiong, Renhe Ji, and Haoqiang Fan. Deep fusion network for image completion. *arXiv preprint arXiv:1904.08060*, 2019.
- [8] Phillip Isola, Jun-Yan Zhu, Tinghui Zhou, and Alexei A Efros. Image-to-image translation with conditional adversarial networks. In *Proceedings of the IEEE Conference on Computer Vision and Pattern Recognition (CVPR)*, pages 1125–1134, 2017.
- [9] Kyong Hwan Jin and Jong Chul Ye. Annihilating filter-based low-rank hankel matrix approach for image inpainting. *IEEE Transactions on Image Processing*, 24(11):3498–3511, 2015.
- [10] Tero Karras, Timo Aila, Samuli Laine, and Jaakko Lehtinen. Progressive growing of GANs for improved quality, stability, and variation. In *International Conference on Learning Representations (ICLR)*, 2018.
- [11] Yijun Li, Sifei Liu, Jimei Yang, and Ming-Hsuan Yang. Generative face completion. In *IEEE Conference on Computer Vision and Pattern Recognition*, 2017.
- [12] Yijun Li, Sifei Liu, Jimei Yang, and Ming-Hsuan Yang. Generative face completion. In *Proceedings of the IEEE Conference on Computer Vision and Pattern Recognition (CVPR)*, pages 3911–3919, 2017.
- [13] Haofu Liao, Gareth Funka-Lea, Yefeng Zheng, Jiebo Luo, and S Kevin Zhou. Face completion with semantic knowledge and collaborative adversarial learning. In *Asian Conference on Computer Vision*, pages 382–397. Springer, 2018.
- [14] Guilin Liu, Fitsum A Reda, Kevin J Shih, Ting-Chun Wang, Andrew Tao, and Bryan Catanzaro. Image inpainting for irregular holes using partial convolutions. In *Proceedings of the European Conference on Computer Vision (ECCV)*, pages 85–100, 2018.
- [15] Ziwei Liu, Ping Luo, Xiaogang Wang, and Xiaoou Tang. Deep learning face attributes in the wild. In *Proceedings of International Conference on Computer Vision (ICCV)*, December 2015.
- [16] Sebastian Lutz, Konstantinos Amliantis, and Aljosa Smolic. Alphagan: Generative adversarial networks for natural image matting. *arXiv preprint arXiv:1807.10088*, 2018.
- [17] Alireza Makhzani, Jonathon Shlens, Navdeep Jaitly, Ian Goodfellow, and Brendan Frey. Adversarial autoencoders. *arXiv preprint arXiv:1511.05644*, 2015.
- [18] Deepak Pathak, Philipp Krahenbuhl, Jeff Donahue, Trevor Darrell, and Alexei A Efros. Context encoders: Feature learning by inpainting. In *Proceedings of the IEEE Conference on Computer Vision and Pattern Recognition (CVPR)*, pages 2536–2544, 2016.
- [19] Yunchen Pu, Zhe Gan, Ricardo Henao, Xin Yuan, Chunyuan Li, Andrew Stevens, and Lawrence Carin. Variational autoencoder for deep learning of images, labels and captions. In *Advances in neural information processing systems*, pages 2352–2360, 2016.
- [20] Yurui Ren, Xiaoming Yu, Ruonan Zhang, Thomas H Li, Shan Liu, and Ge Li. Structureflow: Image inpainting via structure-aware appearance flow. In *Proceedings of the IEEE International Conference on Computer Vision*, pages 181–190, 2019.
- [21] Olaf Ronneberger, Philipp Fischer, and Thomas Brox. U-net: Convolutional networks for biomedical image segmentation. In *International Conference on Medical image computing and computer-assisted intervention*, pages 234–241. Springer, 2015.
- [22] Mihaela Rosca, Balaji Lakshminarayanan, David Warde-Farley, and Shakir Mohamed. Variational approaches for auto-encoding generative adversarial networks. *arXiv preprint arXiv:1706.04987*, 2017.
- [23] Yuhang Song, Chao Yang, Zhe Lin, Xiaofeng Liu, Qin Huang, Hao Li, and C-C Jay Kuo. Contextual-based image inpainting: Infer, match, and translate. In *Proceedings of the European Conference on Computer Vision (ECCV)*, pages 3–19, 2018.

- [24] Patricia Vitoria, Joan Sintes, and Coloma Ballester. Semantic image inpainting through improved wasserstein generative adversarial networks. *arXiv preprint arXiv:1812.01071*, 2018.
- [25] Nannan Wang, Xinbo Gao, Dacheng Tao, Heng Yang, and Xuelong Li. Facial feature point detection: A comprehensive survey. *Neurocomputing*, 275:50–65, 2018.
- [26] Yi Wang, Xin Tao, Xiaojuan Qi, Xiaoyong Shen, and Jiaya Jia. Image inpainting via generative multi-column convolutional neural networks. In *Advances in Neural Information Processing Systems*, pages 331–340, 2018.
- [27] Oliver Whyte, Josef Sivic, and Andrew Zisserman. Get out of my picture! internet-based inpainting. In *British Machine Vision Conference (BMVC)*, volume 2, page 5, 2009.
- [28] Jing Xiao, Liang Liao, Qiegen Liu, and Ruimin Hu. Cisi-net: Explicit latent content inference and imitated style rendering for image inpainting. In *Proceedings of the AAAI Conference on Artificial Intelligence (AAAI)*, volume 33, pages 354–362, 2019.
- [29] Chaohao Xie, Shaohui Liu, Chao Li, Ming-Ming Cheng, Wangmeng Zuo, Xiao Liu, Shilei Wen, and Errui Ding. Image inpainting with learnable bidirectional attention maps. In *Proceedings of the IEEE International Conference on Computer Vision*, pages 8858–8867, 2019.
- [30] Wei Xiong, Jiahui Yu, Zhe Lin, Jimei Yang, Xin Lu, Connelly Barnes, and Jiebo Luo. Foreground-aware image inpainting. In *Proceedings of the IEEE Conference on Computer Vision and Pattern Recognition*, pages 5840–5848, 2019.
- [31] Zongben Xu and Jian Sun. Image inpainting by patch propagation using patch sparsity. *IEEE transactions on image processing*, 19(5):1153–1165, 2010.
- [32] Zhaoyi Yan, Xiaoming Li, Mu Li, Wangmeng Zuo, and Shiguang Shan. Shift-net: Image inpainting via deep feature rearrangement. In *Proceedings of the European Conference on Computer Vision (ECCV)*, pages 1–17, 2018.
- [33] Chao Yang, Xin Lu, Zhe Lin, Eli Shechtman, Oliver Wang, and Hao Li. High-resolution image inpainting using multi-scale neural patch synthesis. In *Proceedings of the IEEE Conference on Computer Vision and Pattern Recognition*, pages 6721–6729, 2017.
- [34] Raymond A Yeh, Chen Chen, Teck Yian Lim, Alexander G Schwing, Mark Hasegawa-Johnson, and Minh N Do. Semantic image inpainting with deep generative models. In *Proceedings of the IEEE Conference on Computer Vision and Pattern Recognition (CVPR)*, pages 5485–5493, 2017.
- [35] Jiahui Yu, Zhe Lin, Jimei Yang, Xiaohui Shen, Xin Lu, and Thomas S Huang. Generative image inpainting with contextual attention. In *Proceedings of the IEEE Conference on Computer Vision and Pattern Recognition (CVPR)*, pages 5505–5514, 2018.
- [36] Jiahui Yu, Zhe Lin, Jimei Yang, Xiaohui Shen, Xin Lu, and Thomas S Huang. Free-form image inpainting with gated convolution. In *Proceedings of the IEEE International Conference on Computer Vision*, pages 4471–4480, 2019.
- [37] Yanhong Zeng, Jianlong Fu, Hongyang Chao, and Baining Guo. Learning pyramid-context encoder network for high-quality image inpainting. In *The IEEE Conference on Computer Vision and Pattern Recognition (CVPR)*, June 2019.
- [38] Haoran Zhang, Zhenzhen Hu, Changzhi Luo, Wangmeng Zuo, and Meng Wang. Semantic image inpainting with progressive generative networks. In *ACM Multimedia Conference on Multimedia Conference (ACM MM)*, pages 1939–1947. ACM, 2018.
- [39] Chuanxia Zheng, Tat-Jen Cham, and Jianfei Cai. Pluralistic image completion. In *Proceedings of the IEEE Conference on Computer Vision and Pattern Recognition (CVPR)*, pages 1438–1447, 2019.